www.dergipark.gov.tr
ISSN:2148-3736
El-Cezerî Fen ve Mühendislik Dergisi
Cilt: 6, No: 3, 2019 (642-658)

El-Cezerî Journal of Science and Engineering
Vol: 6, No: 3, 2019 (642-658)

DOI:10.31202/ecjse.563802

ECJSE

Research Paper / Makale

The contribution of Multi-GNSS Experiment (MGEX) to precise point positioning over Turkey: Consideration of observation time and satellite geometry

Sermet OGUTCU*

Necmettin Erbakan University, Engineering Faculty, 42100 Konya/TÜRKİYE, sermetogutcu@konya.edu.tr

Received/Geliş: 13.05.2019 **Accepted/Kabul:** 06.07.2019

Abstract: In addition to the legacy GPS and GLONASS, new emerging systems, e.g. European Galileo and Chinese BeiDou became operational for positioning, timing and navigation purposes. The International GNSS Service (IGS) has initiated the Multi-GNSS Experiment for adaptation of new emerging systems. An increasing number of satellites of GNSS and their constant modernization allow conducting precise point positioning (PPP) with four constellations, namely GPS, BeiDou, GLONASS and Galileo. In this paper, the performance of quad-constellation PPP over Turkey is investigated using different observation time (24-, 12-, 6-, 3-, and 1-h) and elevation cutoff angles (7°-15°-30°). Ten consecutive days in 2018 (DOY: 324-333) and six IGS-MGEX stations are chosen within and around Turkey to conduct quad-constellation PPP. The results indicate that quad-constellation PPP increases the horizontal and vertical accuracy compared to the GPS only PPP. As the elevation cutoff angle increases, the accuracy improvements are getting higher compared to the unconstrained environment. The improvements in the vertical component are much higher than the horizontal component for most of the stations. The results also reveal that the number of outliers is significantly low for multi-GNSS PPP compared to the GPS only PPP, especially for short observation time.

Keywords: Accuracy, BeiDou, Galileo, GNSS, GPS, PPP

Çoklu-Gnss'in (MGEX) Türkiye Üzerinde Hassas Nokta Konumlandirmasina Katkisi: Gözlem Süresi ve Uydu Geometrisinin Değerlendirilmesi Üzerine Bir Çalışma

Öz: Uydu yörünge sistemini tamamlamış GPS ve GLONASS sistemlerine ilave olarak GALILEO ve BeiDou uydu navigasyon sistemleri tam kapasite uydu yörünge sistemine geçebilmek için hızlı bir şekilde güncellenmektedir. Uluslararası GNSS servisi (IGS) gelişen farklı uydu sistemleri için çoklu-GNSS hizmetini (IGS-MGEX) başlatmıştır. Sayısı artmakta olan özellikle Galileo ve BeiDou uydu navigasyon sistemleri kullanılarak dört farklı küresel navigasyon amaçlı hizmet veren GPS, GLONASS, GALILEO ve BeiDou uyduları kullanılarak hassas nokta konumlama (PPP) yapılabilmektedir. Bu çalışmada GPS, GLONASS, GALILEO ve BeiDou uydularından yararlanılarak (GPS, GPS-GLONASS, GPS-GLONASS-GALILEO ve GPS-GLONASS-GALILEO-BeiDou kombinasyonları ile) farklı oturum süreleri (24-12-6-3-1 saat) ve uydu yüksek açıları (7°-15°-30°) için PPP doğruluk performansı Türkiye ve çevresi için analiz edilmiştir. 20-30 Kasım 2018 tarihleri arasında 10 gün ve altı adet IGS-MGEX istasyonu Türkiye içinde ve çevresinde olmak üzere seçilmiştir. Sonuçlar, çoklu GNSS kullanılarak yapılan PPP değerlendirmelerinde yatay ve düşey doğruluğun tek GPS uydusu kullanılarak yapılan PPP değerlendirmesine göre daha yüksek çıktığını göstermektedir. Özellikle uydu yükseklik açısı artıkça tek GPS sistemine göre çoklu-GNSS değerlendirmesindeki doğruluğun çok daha fazla arttığı gözlemlenmektedir. Çoklu-GNSS değerlendirmesindeki düşey doğruluktaki artışın yatay doğruluğa göre çoğu istasyon için daha fazla olduğu görülmektedir. Sonuçlar aynı zamanda kısa oturum sürelerindeki uyuşumsuz ölçülerin çoklu GNSS kullanılarak önemli oranda azaldığını göstermektedir.

Anahtar kelimeler: Doğruluk, BeiDou, Galileo, GNSS, GPS, PPP

How to cite this article
Ogutcu, S., "*The contribution of Multi-GNSS Experiment (MGEX) to precise point positioning over Turkey: Consideration of observation time and satellite geometry*" El-Cezerî Journal of Science and Engineering, 2019, 6(3); 642-658.

Bu makaleye atıf yapmak için
Ogutcu, S., *"Çoklu-Gnss'in (MGEX) Türkiye Üzerinde Hassas NoktaKonumlandirmasina Katkisi: Gözlem Süresi Ve Uydu Geometrisinin Değerlendirilmesi Üzerine Bir Çalişma"* El-Cezerî Fen ve Mühendislik Dergisi 2019, 6(3); 642-658.

1. Introduction

Precise Point Positioning [1] has become a powerful tool for obtaining precise positioning using precise satellite orbit and clock corrections provided by, for example, International Global Navigation Satellite System (GNSS) service. It plays a key role in much scientific research, such as tectonic and geophysical studies [2-3] and atmosphere and earthquake monitoring [4-5].

One of the main advantages of PPP compared to differential techniques is users can obtain a homogeneous positioning accuracy around the world through PPP using a single receiver without depending on any fiducial stations. Over the past decades, the Global Positioning System (GPS), as the first space-based radio-navigation system for positioning, timing and navigation (PTN). Currently, with two new and emerging constellations (BeiDou, Galileo) as well as the recovery of Russia's GLONASS, the world of satellite navigation is undergoing dramatic changes for more precise and reliable GNSS applications and services [5]. The GLONASS constellation has been fully recovered since October 2011 and is operating at full service capability with 24 satellites in orbits at the moment, enabling full global coverage for PTN (https://www.glonass-iac.ru/en/GLONASS/index.php). Europe's Galileo is the third GNSS, aiming to offer a continuous, precise positioning service globally. The full Galileo constellation will consist of 30 satellites in three orbital planes, including three in-orbit spare ones (http://www.esa.int/Our_Activities/Navigation/The_future_-_Galileo/What_is_Galileo). The BeiDou navigation satellite system, being established independently in China, is pacing steadily forward towards its final full global orbit capability comprises 5 GEO (Geostationary Earth Orbit), 3 IGSO (Inclined Geo-Synchronous Orbit), and 27 MEO (Medium Earth Orbit) satellites by 2020. Once all four systems are fully deployed, about 120 navigation satellites will be available for GNSS users [6]. As for now, BDS-2 has been completed to serve mainly Asian-Pacific regions. Most of the navigation satellites belong to BDS-3 has been launched so far but due to the signal differences a few GNSS stations can record BDS-3 phase and code data. RINEX 3.04 version can consistently record phase and code data of BDS-3 satellites. Moreover, most of the GNSS stations need to be updated for firmware and hardware for working BDS-3 signals consistently (Private communication with CSNO-TARC). To prepare for the next phase of generating satellite and orbit products for all GNSS available, the IGS initiated the IGS Multi-GNSS Experiment (MGEX) campaign [7]. The MGEX campaign focuses on tracking and storing the newly available GNSS signals including the BeiDou and Galileo in addition to GPS and GLONASS. There are numerous research studies addressing the multi-GNSS PPP [8-9-10-11-12]. These studies confirmed that multi-GNSS PPP solutions are more accurate and robust compared to the GPS only PPP solution. Bahadır and Nohutcu, [13] conducted multi-GNSS PPP solutions using with different constellation combinations over Turkey for the first time. The results revealed that multi-GNSS PPP solutions are more accurate than GPS only PPP solutions. Moreover, the results also confirmed that the convergence time of multi GNSS PPP solutions is much shorter than GPS only PPP solutions. The main limitation of this study is that constant observation time (daily) and elevation cutoff angle (not specified in the study) are used to evaluate multi-GNSS PPP solutions. Multi-GNSS PPP solutions over Turkey using different observation time and elevation cutoff angles under poor satellite geometry (such as nearby buildings and street-canyons) are worth to investigate. On the basis of this situation, this paper investigates the performance evaluation of multi-GNSS PPP using with different observation durations (24, 12, 6, 3 and 1 h) and different satellite cutoff elevation angles (7°–15°-30°). This paper is organized as follows. Section 2 describes the PPP functional model, Section 3 presents the data processing. The results are summarized and discussed in Section 4 and the work is concluded in Section 5.

2. PPP Observation Model

In general, ionosphere-free code and carrier phase observations are used for PPP in order to

eliminate the first-order ionosphere effect. The equations can be written for phase and code observations as follows;

$$P^s_{IF,r}=\rho + c*(dt_r - dt^s) + d_{trop} + HD_{P,r,IF} - HD^{P,s,IF} + \epsilon_{P,IF} \quad (1)$$

$$\emptyset^{\mathrm{S}}_{\mathrm{IF,r}} = \rho + \mathrm{c}*(\mathrm{dt_r} - \mathrm{dt^s}) + \mathrm{d_{trop}} + \lambda_{\mathrm{IF}}*\mathrm{N^s_{IF}} + \mathrm{HD_{\emptyset,r,IF}} - \mathrm{HD^{\emptyset,s,IF}} + \epsilon_{\emptyset,\mathrm{if}} \quad (2)$$

where the superscript s represents satellite, the subscript r represents receiver, $P^s_{IF,r}$ and $\emptyset^S_{IF,r}$ are the ionosphere-free combination of code and phase observations, ρ is the geometric range in meters, c is the speed of light in meters per second, dt_r is the receiver clock offset in seconds, dt^s is the satellite clock offset in seconds, d_{trop} is the tropospheric delay in meters, λ_{IF} is the ionosphere-free wavelength, N_{IF} is the ionosphere-free phase initial ambiguity, $HD_{P,r,IF}$ and $HD_{\emptyset,r,IF}$ are the ionosphere-free code and phase receiver hardware delay in meter, $HD^{P,s,IF}$ and $HD^{\emptyset,s,IF}$ are the ionosphere-free code and phase satellite hardware delay in meter and $\epsilon_{P,IF}$ and $\epsilon_{\emptyset,1f}$ are the ionosphere-free code and phase measurement noise. The ionosphere-free code and carrier phase observables can be written as;

$$P^s_{IF,r}= (f1^2 * P1^s - f2^2 * P2^s)/(f1^2 - f2^2) \quad (3)$$

$$\emptyset^s_{IF,r}= (f1^2 * \emptyset1^s - f2^2 * \emptyset2^s)/(f1^2 - f2^2) \quad (4)$$

where f1 and f2 are two carrier-phase frequencies in Hertz and P1, P2, ∅1, ∅1 are the measured pseudorange and carrier phase in meters on two frequencies. Ionosphere-free wavelength and ionosphere-free ambiguity can be written as;

$$\lambda_{IF} = \frac{f1^2}{f1^2-f2^2} * \lambda_1 - \frac{f2^2}{f1^2-f2^2} * \lambda_2 \quad (5)$$

$$N_{IF}=\frac{f1^2*N_1}{f1^2-f2^2} - \frac{f2^2*N_2}{f1^2-f2^2} \quad (6)$$

where N1 and N2 are the phase initial integer ambiguities on two frequencies with respect to each observed satellite. As it is seen from Equation 6, ionosphere-free ambiguity can only be estimated as a float (real-value) unknown unless using bias information from the network. For PPP users, the receiver dependent HD is generally not a concern and can be safely ignored [14]. Using the above equations and considering GPS time as a reference time system, the un-differenced ionosphere-free linear combinations of GPS, GLONASS, Galileo and BeiDou observations can be written as [15]:

$$P^G_{IF,r} = \rho_G + c*(dt_r - dt^s) + d^G_{trop} + HD_{P,r,IF} - HD^{P,G,IF} + \epsilon^G_{P,IF} \quad (7)$$

$$P^R_{IF,r} = \rho_R + c*(dt_r - dt^s + ISB^R) + d^R_{trop} + HD_{P,r,IF} - HD^{P,R,IF} + \epsilon^R_{P,IF} \quad (8)$$

$$P^E_{IF,r} = \rho_E + c*(dt_r - dt^s + ISB^E) + d^E_{trop} + HD_{P,r,IF} - HD^{P,E,IF} + \epsilon^E_{P,IF} \quad (9)$$

$$P^C_{IF,r} = \rho_C + c*(dt_r - dt^s + ISB^C) + d^C_{trop} + HD_{P,r,IF} - HD^{P,C,IF} + \epsilon^C_{P,IF} \quad (10)$$

$$\emptyset^G_{IF,r} = \rho_G + c*(dt_r - dt^s) + d^G_{trop} + (\lambda_{IF} * N^G_{IF}) + HD_{\emptyset,r,IF} - HD^{\emptyset,G,IF} + \epsilon^G_{P,IF} \quad (11)$$

$$\emptyset^R_{IF,r} = \rho_R + c*(dt_r - dt^s + ISB^R) + d^R_{trop} + (\lambda_{IF} * N^R_{IF}) + HD_{\emptyset,r,IF} - HD^{\emptyset,R,IF} + \epsilon^R_{P,IF} \quad (12)$$

$$\emptyset^E_{IF,r} = \rho_E + c*(dt_r - dt^s + ISB^E) + d^E_{trop} + (\lambda_{IF} * N^E_{IF}) + HD_{\emptyset,r,IF} - HD^{\emptyset,E,IF} + \epsilon^E_{P,IF} \quad (13)$$

$$\emptyset_{IF,r}^{C} = \rho_C + c * (dt_r - dt^s + ISB^C) + d_{trop}^{C} + (\lambda_{IF} * N_{IF}^{C}) + HD_{\emptyset,r,IF} - HD^{\emptyset,C,IF} + \epsilon_{P,IF}^{C} \quad (14)$$

where G, R, E and C refer to GPS, GLONASS, Galileo and BeiDou systems observations respectively; ISB can be explained as sum of receiver-dependent hardware delay differences occurring among different GNSSs and the receiver-independent time differences caused by different clock datum constraints among external GNSS satellite clock products [16]. As can be seen from Equations 11-14, uncalibrated ionosphere-free hardware delays are lumped with the ambiguity parameters.

3. Data Processing

Ten consecutive days in 2018 (DOY: 324-333) and six IGS-MGEX stations are chosen within and around Turkey to conduct quad-constellation PPP. Figure 1 shows the location of the IGS-MGEX stations.

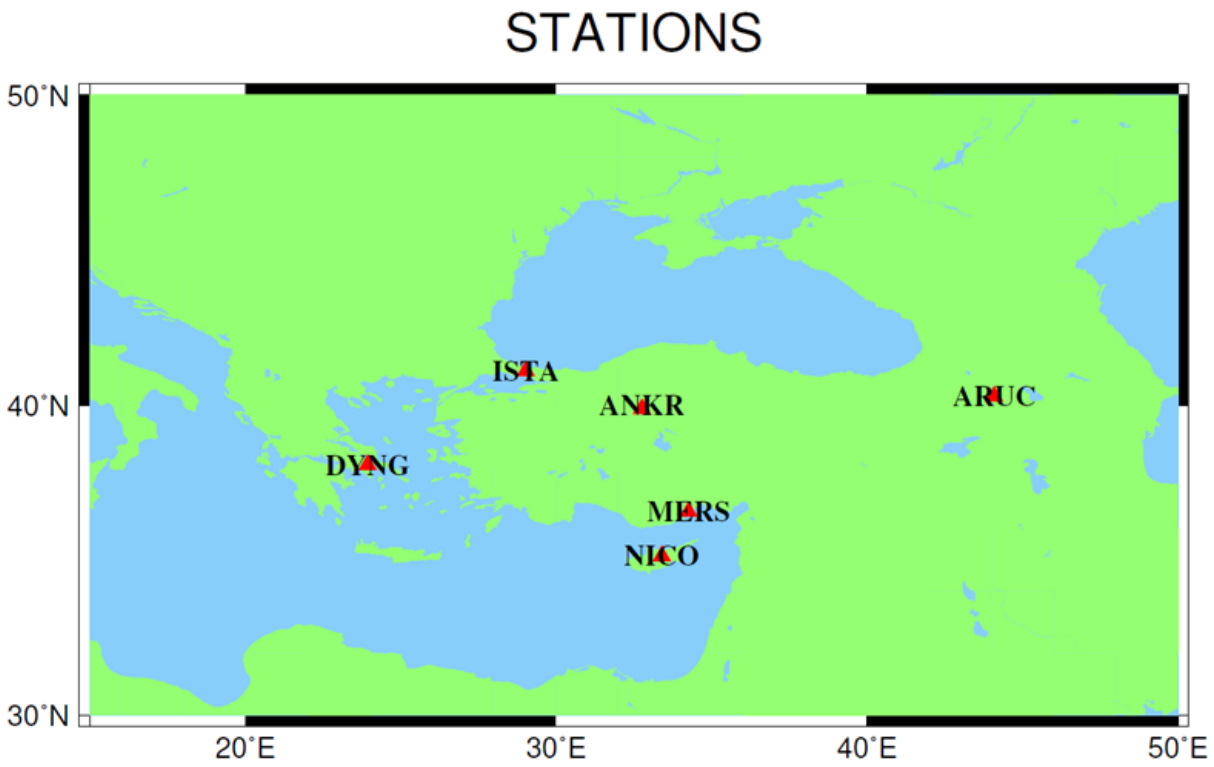

Figure 1. Location of the IGS-MGEX stations

Figure 2 shows the mean values of satellites visibility of IGS-MGEX stations.

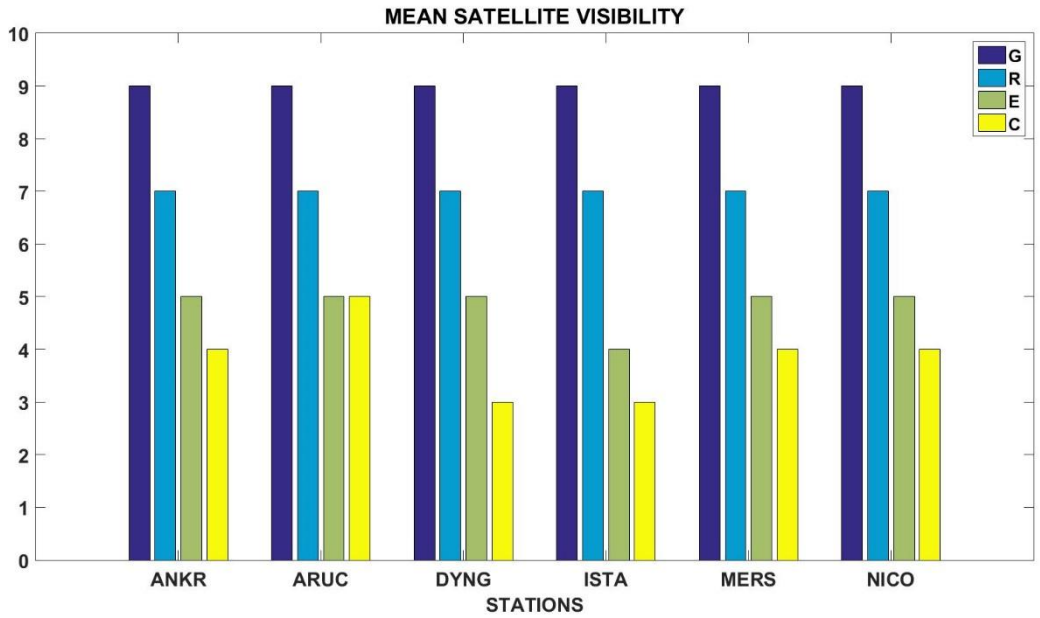

Figure 2. Mean satellite visibility per epoch for each IGS-MGEX station (cutoff: 7°)

As it is seen in Figure 2, mean satellite visibility of GPS and GLONASS is identical for each station. Mean satellite visibility of GALILEO is five for each station except for ISTA station. ISTA station has four mean GALILEO satellite visibility. BeiDou satellite visibility is fluctuating between three and five among the stations. BDS-3 and BDS-2 GEO satellites are not included when computing satellite visibility. Each day's 24 h Receiver Independent Exchange (RINEX) data were mutually subdivided into 24-12-6-3-1 hours of non-overlapping sessions for each station. As a result, 10, 20, 40, 80 and 240 PPP processing were conducted for 24-12-6-3-1 h subdivided RINEX data for each cutoff angle and station, respectively. Daily rinex files data integrity was checked using the software developed by the author. It is found that data integrity is more than 97 % for each file. Each subdivided data were processed using 7°-15°-30° elevation cutoff angles. PPP was conducted for each station as GPS (G) only, GPS+GLONASS (GR), GPS+GLONASS+GALILEO (GRE), and GPS+GLONASS+GALILEO+ BeiDou (GREC). Table 1 shows the average dilution of precision (DOP) values of GNSS constellations during the survey period for 7° elevation cutoff.

Table 1. Average DOP values of GNSS constellations

STATIONS		GDOP	PDOP	HDOP	VDOP
ANKR	G	1.9	1.7	1.0	1.4
	R	2.6	2.3	1.2	1.9
	E	3.6	3.4	2.2	2.8
	C	8.1	6.8	4.3	5.2
	GREC	1.1	1.0	0.5	0.8
ARUC	G	1.9	1.7	0.9	1.4
	R	2.4	2.2	1.1	1.8
	E	3.6	3.2	2.0	2.4
	C	2.1	1.8	1.0	1.5
	GREC	0.9	0.8	0.5	0.7
DYNG	G	2.0	1.8	1.0	1.5
	R	2.5	2.2	1.1	1.9
	E	3.8	3.4	2.0	2.6
	C	7.7	6.6	4.3	4.8
	GREC	1.1	1.0	0.5	0.8
ISTA	G	2.0	1.7	1.0	1.4
	R	2.6	2.3	1.2	1.9
	E	9.2	8.3	4.6	6.9
	C	7.2	6.4	4.8	5.8
	GREC	1.2	1.1	0.6	0.9
MERS	G	2.0	1.7	1.0	1.4
	R	2.7	2.3	1.2	2.0
	E	3.8	3.5	2.3	2.8
	C	8.0	6.7	4.2	5.1
	GREC	1.1	1.0	0.5	0.8
NICO	G	2.0	1.7	1.0	1.4
	R	2.6	2.3	1.2	2.0
	E	4.0	3.5	2.1	2.7
	C	7.6	6.4	3.9	4.9
	GREC	1.1	1.0	0.5	0.8

As it is seen in Table 1, multi-GNSS constellation significantly improves the DOP values for each station compared to the single system. Table 2 summarizes the PPP processing strategy.

Table 2. PPP processing strategy

Item	Descriptions
Software	GipsyX
Adjustment Model	Stochastic Kalman filter/smoother implemented as square root information filter with smoother
Filter	Forward and backward smoothing
Satellite and Orbit Products	Fix to CODE final product Interval: Satellite orbit: 15 min; Satellite clock: 5 min
Reference Frame Realization	Fix to satellites CODE coordinates (IGS14)
GNSS System	GPS, GPS/GLONASS, GPS/GLONASS/GALILEO, GPS/GLONASS/GALILEO/ BeiDou (except for GEO satellites)
Frequencies (Phase and code)	GPS: L1C/L2W/C1C/C2W GLONASS: L1C/L2P/C1P/C2P GALILEO_1:L1C/L7Q/C1C/C7Q GALILEO_2: L1X/L7X/C1X/C7X BeiDou: L2I/L7I/C2I/C7I
Epoch Interval	30 s
Elevation cutoff angle	7°-15°-30°
Weighting Strategy	A priori precision of 0.01 and 0.1 m for raw phase and code for GPS, GALILEO, BeiDou (MEO) and BeiDou (IGSO). GLONASS a priori code precision:1.5 m Elevation dependent weighting: 1/sin(E)
Receiver and Satellite Phase Center	PCO and PCV values for GPS and GLONASS from igs14.atx are used; Corrections for BeiDou and GALILEO are assumed the same with GPS
Ionospheric Effect	First order was removed by ionosphere free linear combination, second order was removed using JPL IONEX file
Phase Ambiguities	Estimated as float constants for each arc unless cycle slips introduces
Inter-System biases	GALILEO, BeiDou: Estimated as random walk for each epoch of all constellations GLONASS: Estimated as random walk for each epoch of all satellites
Intra-Frequency Bias	GPS C1-P1 code bias was corrected using up-to-date DCB file.
A priori troposphere	GPT2 model [17]
Zenith wet delay estimation	random walk 0.05 mm km/sqrt(sec)
Horizontal delay gradients estimation	random walk 0.005 mm/sqrt(sec)
Phase windup	Corrected [18]
Tidal effects	Considering solid tides, ocean loading and polar tides [IERS 2010; 19]
Relativistic corrections	Periodic clock corrections and gravitational bending (shapiro delay) were applied
Cycle-slip	Corrected by Melborne-Wubbena combination.
Receiver clock jump	Corrected
Eclipse strategy	Eclipsing satellites were not used until satellites reach nominal attitude

Since the orbit and clock accuracy of BeiDou GEO satellites are much worse compared to MEO and IGSO satellites, BeiDou GEO satellites are not included in the PPP processing. Even assigning low-weigh of GEO cannot improve the accuracy and convergence time [20; 21]. Due to the effect of GLONASS inter-frequency code bias (IFCB) arises from frequency division multiple access (FDMA), code observations of GLONASS down-weighted as 1.5 m. ISB was determined for GALILEO and BeiDou constellations as a whole but it was determined for each GLONASS satellites due to the FDMA nature.

4. Results

The reference coordinates of the stations were taken from IGS weekly combined solutions with an accuracy of within a few millimeters for the computation of root mean squared error (RMSE). If any coordinate component's error with regards to the true solution was greater than 10 cm, it was assumed to be an outlier but included to RMSE computation for intuitive comparison. The below tables summarize the processing results as two-dimensional and vertical RMSE and the coordinates improvement of multi-GNSS solutions with regards to GPS only solutions. Negative sign of improvement represents the accuracy degradation compared to GPS only solutions.

Table 3. Statistical values for 7° cutoff angle

		24 h						**12 h**					
		RMSE (mm)				**Improvement (mm)**		**RMSE (mm)**				**Improvement (mm)**	
Sites	**Constellation**	**n**	**e**	**u**	**2D**	**2D**	**Up**	**n**	**e**	**u**	**2D**	**2D**	**Up**
ANKR	G	3.8	1.5	7.7	4.1			4.0	3.3	8.9	5.2		
	GR	4.3	3.8	4.3	5.8	**-1.7**	**3.4**	4.4	4.1	4.7	6.0	**-0.8**	**4.2**
	GRE	4.0	4.0	7.1	5.6	**-1.5**	**0.6**	4.1	4.1	7.5	5.8	**-0.6**	**1.4**
	GREC	3.3	1.4	8.5	3.5	**0.6**	**-0.8**	3.3	1.8	8.1	3.8	**1.4**	**0.8**
ARUC	G	3.0	4.0	15.7	5.0			3.2	4.1	15.6	5.2		
	GR	4.1	1.5	6.5	4.3	**0.7**	**9.2**	4.1	1.7	7.1	4.5	**0.7**	**8.5**
	GRE	3.8	1.0	1.2	3.9	**1.1**	**14.5**	3.9	1.4	3.3	4.1	**1.1**	**12.3**
	GREC	3.9	1.6	1.2	4.2	**0.8**	**14.5**	3.9	1.5	4.0	4.2	**1.0**	**11.6**
DYNG	G	6.9	2.6	13.8	7.3			7.5	4.1	14.7	8.6		
	GR	6.9	3.9	8.3	7.9	**-0.6**	**5.5**	7.3	4.8	9.1	8.8	**-0.2**	**5.6**
	GRE	6.8	5.0	5.5	8.4	**-1.1**	**8.3**	7.2	5.5	6.6	9.1	**-0.5**	**8.1**
	GREC	6.7	3.1	7.1	7.3	**0.0**	**6.7**	6.9	3.5	7.3	7.8	**0.8**	**7.4**
ISTA	G	4.4	2.4	9.1	5.0			4.6	3.2	10.2	5.6		

	GR	4.8	1.0	2.6	4.9	**0.1**	**6.5**	4.9	1.7	4.3	5.2	**0.4**	**5.9**
	GRE	4.5	1.1	3.6	4.6	**0.4**	**5.5**	4.6	1.6	5.1	4.9	**0.7**	**5.1**
	GREC	4.4	1.2	4.5	4.6	**0.4**	**4.6**	4.5	1.7	6.0	4.8	**0.8**	**4.2**
MERS	G	4.7	4.4	10.6	6.5			4.9	4.0	12.0	6.3		
	GR	4.3	2.8	7.9	5.1	**1.4**	**2.7**	4.4	2.4	9.4	5.0	**1.3**	**2.6**
	GRE	3.7	2.9	4.2	4.7	**1.8**	**6.4**	3.9	2.5	6.1	4.6	**1.7**	**5.9**
	GREC	3.5	4.0	4.8	5.3	**1.2**	**5.8**	3.7	3.0	6.3	4.8	**1.5**	**5.7**
NICO	G	5.6	1.7	6.7	5.8			5.6	3.2	8.4	6.4		
	GR	5.4	1.4	4.9	5.6	**0.2**	**1.8**	5.5	1.9	6.3	5.8	**0.6**	**2.1**
	GRE	4.7	1.3	6.6	4.9	**0.9**	**0.1**	4.9	1.5	7.9	5.1	**1.3**	**0.5**
	GREC	4.3	2.3	9.5	4.9	**0.9**	**-2.8**	4.5	2.0	10.3	4.9	**1.5**	**-1.9**
		6 h						**3 h**					
		RMSE (mm)				**Improvement (mm)**		**RMSE (mm)**				**Improvement (mm)**	
Sites	**Constellation**	**n**	**e**	**u**	**2D**	**2D**	**Up**	**n**	**e**	**u**	**2D**	**2D**	**Up**
ANKR	G	3.6	7.7	6.5	8.4			5.8	12.2	10.8	13.5		
	GR	5.0	4.2	5.8	6.5	**1.9**	**0.7**	5.0	6.1	8.4	7.9	**5.6**	**2.4**
	GRE	4.8	4.5	7.8	6.5	**1.9**	**-1.3**	4.8	5.4	9.7	7.2	**6.3**	**1.1**
	GREC	4.0	3.7	9.3	5.4	**3.0**	**-2.8**	4.4	4.4	10.5	6.2	**7.3**	**0.3**
ARUC	G	3.0	7.0	17.3	7.6			2.8	10.6	20.0	11.0		
	GR	4.8	3.3	8.6	5.9	**1.7**	**8.7**	4.6	6.7	9.5	8.1	**2.9**	**10.5**
	GRE	4.6	3.5	4.8	5.8	**1.8**	**12.5**	4.4	6.7	7.3	8.0	**3.0**	**12.7**
	GREC	4.6	2.8	5.4	5.4	**2.2**	**11.9**	4.2	6.2	7.4	7.5	**3.5**	**12.6**
DYNG	G	7.5	5.4	15.4	9.2			27.3	20.0	15.0	33.8		
	GR	7.9	5.7	11.0	9.7	**-0.5**	**4.4**	27.0	17.9	13.0	32.4	**1.4**	**2.0**
	GRE	7.9	5.8	8.7	9.8	**-0.6**	**6.7**	27.0	17.7	11.5	32.2	**1.6**	**3.5**
	GREC	7.5	4.7	9.2	8.8	**0.4**	**6.2**	26.8	17.7	11.8	32.1	**1.7**	**3.2**

ISTA	G	4.3	4.0	10.0	5.8			6.0	10.8	12.0	12.4		
	GR	5.3	2.2	6.2	5.8	**0.0**	**3.8**	5.0	4.7	8.9	6.8	**5.6**	**3.1**
	GRE	5.1	2.1	6.1	5.5	**0.3**	**3.9**	4.7	4.9	9.0	6.7	**5.7**	**3.0**
	GREC	5.0	2.2	7.1	5.4	**0.4**	**2.9**	4.6	4.9	9.3	6.7	**5.7**	**2.7**
MERS	G	4.4	5.6	9.6	7.2			6.6	11.3	17.0	13.1		
	GR	4.8	3.2	10.2	5.8	**-1.4**	**-0.6**	5.0	6.0	11.8	7.8	**5.3**	**5.2**
	GRE	4.4	3.7	7.3	5.7	**1.5**	**2.3**	4.9	6.6	9.1	8.2	**4.9**	**7.9**
	GREC	4.3	3.3	7.5	5.4	**1.8**	**2.1**	4.7	5.6	9.2	7.3	**5.8**	**7.8**
NICO								5.5	11.7	13.2	13.0		
	G	5.3	6.0	9.2	8.0			6.2	5.8	15.3	8.5	**4.5**	**-2.1**
	GR	5.7	2.9	9.7	6.4	**1.6**	**-0.5**	6.3	6.1	15.6	8.8	**4.2**	
	GRE	5.2	3.1	10.6	6.1	**1.9**	**-1.4**	6.2	5.7	14.9	8.4	**4.6**	**-2.6**
	GREC	4.9	2.9	12.1	5.7	**2.3**	**-2.9**						**-1.7**

		1 h						
		RMSE (mm)				**Improvement (mm)**		
Sites	**Constellation**	**n**	**e**	**u**	**2D**	**2D**	**Up**	**Outliers**
ANKR	G	13.1	34.2	44.6	36.6			16
	GR	9.6	14.2	18.7	17.1	**19.5**	**25.9**	-
	GRE	8.7	13.6	16.4	16.1	**20.5**	**28.2**	-
	GREC	8.3	13.1	16.7	15.5	**21.1**	**27.9**	-
ARUC	G	23.3	47.3	57.5	52.7			31
	GR	9.6	15.7	17.6	18.4	**34.3**	**39.9**	-
	GRE	9.0	15.1	16.4	17.6	**35.1**	**41.1**	-
	GREC	9.2	14.5	17.0	17.2	**35.5**	**40.5**	-
DYNG	G	29.4	48.7	61.8	56.9			22
	GR	24.1	22.3	23.5	32.9	**24.0**	**38.3**	1
	GRE	23.9	20.8	20.0	31.6	**25.3**	**41.8**	-
	GREC	23.9	19.9	20.5	31.2	**25.7**	**41.3**	-
ISTA	G	15.2	31.0	44.6	34.5			9

	GR	9.9	15.8	20.0	18.6	**15.9**	**24.6**	1
	GRE	9.2	15.3	18.4	17.8	**16.7**	**26.2**	-
	GREC	8.8	14.8	17.8	17.2	**17.3**	**26.8**	-
MERS	G	16.4	43.5	52.2	46.5			16
	GR	9.9	16.8	23.5	19.5	**27.0**	**28.7**	-
	GRE	9.5	15.6	23.6	18.3	**28.2**	**28.6**	-
	GREC	9.1	15.0	22.9	17.6	**28.9**	**29.3**	-
NICO	G	16.1	40.5	51.7	43.6			10
	GR	10.7	16.9	23.3	20.0	**23.6**	**28.4**	4
	GRE	9.4	16.4	23.2	18.9	**24.7**	**28.5**	1
	GREC	9.2	15.3	23.2	17.9	**25.7**	**28.5**	1

Table 4. Statistical values for 15° cutoff angle

		24 h						**12 h**					
		RMSE (mm)				**Improvement (mm)**		**RMSE (mm)**				**Improvement (mm)**	
Sites	**Constellation**	**n**	**e**	**u**	**2D**	**2D**	**Up**	**n**	**e**	**u**	**2D**	**2D**	**Up**
ANKR	G	4.7	2.1	27.3	5.2			5.0	4.2	28.0	6.5		
	GR	4.8	1.1	18.6	5.0	**0.2**	**8.7**	4.8	1.7	18.8	5.1	**1.4**	**9.2**
	GRE	4.7	1.4	8.9	4.9	**0.3**	**8.5**	4.8	1.9	9.3	5.2	**1.3**	**18.7**
	GREC	4.0	3.6	4.4	5.4	**-0.2**	**22.9**	4.1	3.4	5.1	5.3	**1.2**	**22.9**
ARUC	G	3.2	4.2	27.5	5.3			3.5	4.1	27.8	5.4		
	GR	4.1	2.6	17.2	4.9	**0.4**	**10.3**	4.2	2.5	17.5	4.9	**0.5**	**10.3**
	GRE	3.7	1.9	8.6	4.2	**1.1**	**18.9**	3.9	1.7	9.4	4.2	**1.2**	**18.4**
	GREC	3.7	3.0	7.0	4.8	**0.5**	**20.5**	3.9	2.5	8.2	4.6	**0.8**	**19.6**
DYNG	G	6.2	2.6	27.2	6.7			7.0	3.8	27.7	7.9		
	GR	6.1	3.0	18.9	6.8	**-0.1**	**8.3**	6.6	4.0	19.4	7.7	**0.2**	**8.3**
	GRE	5.9	3.2	11.0	6.7	**0.0**	**16.2**	6.3	3.9	12.1	7.4	**0.5**	**15.6**
	GREC	5.4	3.1	8.2	6.2	**0.5**	**19.0**	5.6	3.4	9.3	6.6	**1.3**	**18.4**
ISTA	G	4.1	1.9	24.4	4.5			4.4	3.2	24.3	5.5		
	GR	4.6	0.6	16.8	4.7	**-0.2**	**7.6**	4.8	1.3	17.3	5.0	**0.5**	**7.0**
	GRE	4.4	1.0	9.8	4.5	**0.0**	**14.6**	4.5	1.6	11.0	4.8	**0.7**	**13.3**
	GREC	4.2	1.0	8.5	4.3	**0.2**	**15.9**	4.3	1.5	9.8	4.6	**0.9**	**14.5**
MERS	G	6.6	6.7	6.1	5.6			6.9	4.5	25.7	8.3		
	GR	4.0	2.8	3.0	5.1	**0.4**	**8.4**	6.7	2.6	16.9	7.2	**1.1**	**8.8**
	GRE	24.0	15.6	7.0	3.6	**0.8**	**17.0**	6.2	2.2	8.8	6.6	**1.7**	**16.9**
	GREC	7.7	7.3	6.9	7.6	**0.1**	**20.4**	5.6	3.9	5.8	6.8	**1.5**	**19.9**
NICO	G	5.1	1.9	21.6	5.4			5.2	5.0	4.6	4.0		

	GR	4.9	1.2	15.1	5.0	**0.4**	**6.5**	3.2	1.8	1.6	2.5	**0.8**	**6.5**
	GRE	4.4	1.1	7.4	4.5	**0.9**	**14.2**	22.4	15.9	9.1	5.7	**1.3**	**13.3**
	GREC	3.8	3.0	3.2	4.9	**0.6**	**18.4**	6.1	5.3	4.8	4.7	**1.4**	**16.7**
		6 h						**3 h**					
		RMSE (mm)				**Improvement (mm)**		**RMSE (mm)**				**Improvement (mm)**	
Sites	**Constellation**	**n**	**e**	**u**	**2D**	**2D**	**Up**	**n**	**e**	**u**	**2D**	**2D**	**Up**
ANKR	G	4.8	8.5	24.5	9.8			6.1	11.8	21.7	13.3		
	GR	5.3	3.2	19.4	6.2	**3.6**	**5.1**	5.3	4.9	17.2	7.2	**6.1**	**4.5**
	GRE	5.2	3.6	10.3	6.4	**3.8**	**14.2**	5.3	4.8	11.3	7.1	**6.2**	**10.4**
	GREC	4.6	4.1	7.2	6.1	**3.7**	**17.3**	4.8	4.7	9.8	6.7	**6.6**	**11.9**
ARUC	G	3.4	6.5	27.8	7.3			3.9	11.5	30.7	12.1		
	GR	4.7	3.3	18.7	5.7	**1.6**	**9.1**	4.9	6.2	21.2	8.0	**4.1**	**9.5**
	GRE	4.5	3.5	11.3	5.7	**1.6**	**16.5**	4.6	6.3	15.7	7.8	**4.3**	**15.0**
	GREC	4.4	3.3	9.6	5.5	**1.8**	**18.2**	4.3	5.8	7.2	7.2	**4.9**	**17.3**
DYNG	G	7.0	5.3	27.9	8.9			27.3	21.5	22.7	34.8		
	GR	6.8	5.3	20.8	8.6	**0.3**	**7.1**	26.9	17.8	20.0	32.2	**2.6**	**2.7**
	GRE	6.6	4.7	13.7	8.1	**0.8**	**14.2**	26.8	17.4	15.0	32.0	**2.8**	**7.7**
	GREC	6.1	4.3	11.8	7.4	**1.5**	**16.1**	26.7	17.5	13.7	31.9	**2.9**	**9.0**
ISTA	G	4.4	3.1	24.4	5.4			6.4	11.8	22.3	13.4		
	GR	5.1	2.0	19.5	5.5	**-0.1**	**4.9**	4.7	4.6	6.6	6.6	**6.8**	**4.5**
	GRE	4.8	2.3	12.3	5.4	**0.0**	**12.1**	4.5	5.2	6.9	6.9	**6.7**	**8.8**
	GREC	4.7	2.4	11.5	5.3	**0.1**	**12.9**	4.3	5.0	6.6	6.6	**6.8**	**9.7**
MERS	G	6.0	8.3	20.6	10.3			6.5	14.0	19.9	15.5		
	GR	6.9	3.0	17.4	7.6	**2.7**	**3.2**	6.3	6.7	15.8	9.2	**6.3**	**4.1**
	GRE	6.6	3.3	9.9	7.4	**2.9**	**10.7**	6.2	7.2	12.0	9.5	**6.0**	**7.9**
	GREC	6.2	3.3	8.3	7.0	**3.3**	**11.7**	6.0	6.0	10.9	8.5	**6.5**	**9.0**
NICO	G	5.1	6.2	20.5	8.0			6.1	13.5	21.7	14.8		
	GR	5.2	3.1	16.7	6.0	**2.0**	**3.8**	5.1	5.2	17.4	7.3	**7.5**	**4.3**
	GRE	4.8	3.5	10.4	5.9	**2.1**	**10.1**	5.3	5.4	13.2	7.6	**7.2**	**8.5**
	GREC	4.3	3.3	6.9	5.4	**2.6**	**13.6**	5.2	5.6	11.0	7.6	**7.2**	**10.7**

		1 h						
		RMSE (mm)				**Improvement (mm)**		
Sites	**Constellation**	**n**	**e**	**u**	**2D**	**2D**	**Up**	**Outliers**
ANKR	G	23.7	70.1	80.6	74.0			52
	GR	9.8	14.0	25.1	17.1	**56.9**	**55.5**	1
	GRE	9.0	13.9	18.4	16.5	**57.5**	**62.2**	-
	GREC	8.9	13.7	18.4	16.3	**57.7**	**62.2**	-
ARUC	G	43.6	78.5	104.1	89.8			65
	GR	10.0	15.3	28.9	18.3	**71.5**	**75.2**	-
	GRE	9.4	14.1	25.2	16.9	**72.9**	**78.9**	-
	GREC	9.8	13.8	25.3	16.9	**72.9**	**79.0**	-
DYNG	G	42.5	101.6	155.6	110.1			70
	GR	24.1	23.7	29.5	33.8	**76.3**	**126.1**	1
	GRE	23.7	20.3	22.7	31.2	**78.9**	**132.9**	-
	GREC	23.6	19.7	22.1	30.8	**79.3**	**133.5**	-
ISTA	G	22.9	67.5	60.2	71.3			37

	GR	10.5	15.4	29.0	18.7	**52.6**	**31.2**	-
	GRE	9.4	14.9	23.0	17.7	**53.6**	**37.2**	-
	GREC	9.1	15.2	22.5	17.7	**53.6**	**37.7**	-
MERS	G	21.3	68.3	91.9	71.5			62
	GR	11.5	16.5	27.5	20.2	**51.3**	**64.4**	-
	GRE	10.1	16.1	19.0	19.0	**52.5**	**72.9**	-
	GREC	9.9	15.0	24.3	18.0	**53.5**	**73.9**	-
NICO	G	23.3	71.7	83.6	75.4			61
	GR	10.2	16.2	30.4	19.2	**56.2**	**53.2**	4
	GRE	9.1	15.5	24.6	17.9	**57.5**	**59.0**	1
	GREC	9.1	15.6	24.1	18.1	**57.3**	**59.5**	1

Table 5. Statistical values for 30° cutoff angle

		24 h						**12 h**					
		RMSE (mm)				**Improvement (mm)**		**RMSE (mm)**				**Improvement (mm)**	
Sites	**Constellation**	**n**	**e**	**u**	**2D**	**2D**	**Up**	**n**	**e**	**u**	**2D**	**2D**	**Up**
ANKR	G	4.2	7.4	66.3	8.5			4.4	9.7	69.3	10.6		
	GR	4.5	2.9	46.2	5.3	**3.2**	**20.1**	4.6	3.4	46.8	5.7	**4.9**	**22.5**
	GRE	4.1	1.1	25.9	4.2	**4.3**	**40.4**	4.4	2.2	26.2	5.0	**5.6**	**43.1**
	GREC	3.6	1.4	20.0	3.9	**4.6**	**46.3**	3.9	2.2	20.4	4.5	**6.1**	**48.9**
ARUC	G	2.1	5.7	51.4	6.1			2.7	6.4	62.1	6.9		
	GR	3.0	2.6	32.9	3.9	**2.2**	**18.5**	3.3	3.3	35.1	4.7	**2.2**	**27.0**
	GRE	2.5	1.2	12.8	2.8	**3.3**	**38.6**	3.2	2.8	14.5	4.2	**2.7**	**47.6**
	GREC	2.4	2.1	7.4	3.2	**2.9**	**44.0**	3.2	2.7	11.4	4.2	**2.7**	**50.7**
DYNG	G	4.1	3.5	61.3	5.4			4.5	3.6	62.8	5.8		
	GR	3.1	2.6	38.4	4.1	**1.3**	**22.9**	3.7	3.8	38.9	5.3	**0.5**	**23.9**
	GRE	3.4	3.9	20.7	5.1	**0.3**	**20.7**	3.8	4.5	21.8	5.9	**-0.1**	**21.8**
	GREC	3.0	3.9	17.9	4.9	**0.5**	**43.4**	3.4	4.4	18.8	5.6	**0.2**	**18.8**
ISTA	G	2.6	3.8	43.4	4.6			2.8	3.9	44.1	4.8		
	GR	4.3	1.3	38.3	4.6	**0.0**	**5.1**	4.6	1.9	39.6	5.0	**-0.2**	**4.5**
	GRE	4.1	2.0	19.4	4.5	**0.1**	**24.0**	4.3	2.9	20.9	5.2	**-0.4**	**23.2**
	GREC	3.9	2.1	15.5	4.5	**0.0**	**27.9**	4.1	2.8	17.1	5.0	**-0.2**	**27.0**
MERS	G	9.6	7.2	88.1	12.0			8.8	9.3	78.9	12.8		
	GR	5.9	4.7	56.7	7.6	**4.4**	**31.4**	6.1	5.0	58.1	7.9	**4.9**	**20.8**
	GRE	5.8	4.2	36.5	7.1	**4.9**	**51.6**	5.8	3.9	37.8	7.0	**5.8**	**41.1**
	GREC	5.5	4.7	30.7	7.2	**4.8**	**57.4**	5.6	4.5	32.0	7.1	**5.7**	**46.9**
NICO	G	7.3	3.7	39.6	8.2			7.8	6.0	41.2	9.9		
	GR	6.4	2.1	42.4	6.8	**1.4**	**-2.8**	6.7	3.3	43.6	7.5	**2.4**	**-2.4**
	GRE	6.0	2.0	22.4	6.4	**1.8**	**17.2**	6.3	3.1	23.5	7.0	**2.9**	**17.7**
	GREC	5.7	1.6	17.8	5.9	**2.3**	**21.8**	5.8	2.2	18.9	6.2	**3.7**	**22.3**

		6 h						**3 h**					
		RMSE (mm)				**Improvement (mm)**		**RMSE (mm)**				**Improvement (mm)**	
Sites	**Constellation**	**n**	**e**	**u**	**2D**	**2D**	**Up**	**n**	**e**	**u**	**2D**	**2D**	**Up**
ANKR	G	6.0	12.5	61.1	13.9			9.7	19.5	45.4	21.8		

	GR	5.0	5.1	47.8	7.2	**6.7**	**13.3**	6.1	6.8	44.5	9.1	**12.7**	**0.9**
	GRE	4.8	5.3	27.9	7.2	**6.7**	**33.2**	5.7	6.8	31.8	8.9	**12.9**	**13.6**
	GREC	4.4	4.8	24.3	6.5	**7.4**	**36.8**	5.3	6.0	30.8	8.0	**13.8**	**14.6**
ARUC	G	4.3	10.1	40.4	10.9			6.9	14.6	48.5	16.2		
	GR	3.8	4.4	40.1	5.8	**5.1**	**0.3**	4.7	7.5	50.2	8.9	**7.3**	**-1.7**
	GRE	3.9	4.7	21.6	6.1	**4.8**	**18.8**	5.1	8.3	39.7	9.7	**6.5**	**8.8**
	GREC	3.7	3.7	20.0	5.1	**5.8**	**20.4**	4.8	8.0	34.8	9.3	**6.9**	**13.7**
DYNG	G	6.4	16.7	59.0	17.9			30.7	33.4	42.9	45.3		
	GR	4.1	6.5	41.5	7.7	**10.2**	**17.5**	27.3	18.3	37.5	32.8	**12.5**	**5.4**
	GRE	4.0	7.3	23.5	8.3	**9.6**	**35.5**	26.7	18.0	30.8	32.2	**13.1**	**12.1**
	GREC	3.8	6.9	21.6	7.8	**10.1**	**37.4**	26.5	17.8	29.9	32.0	**13.2**	**13.0**
ISTA	G	4.1	8.9	47.4	9.8			8.0	18.7	46.3	20.3		
	GR	4.7	3.7	41.9	6.0	**3.8**	**5.5**	5.1	6.9	39.4	8.5	**11.8**	**6.9**
	GRE	4.5	4.7	22.3	6.5	**3.3**	**25.1**	5.1	7.8	29.0	9.3	**11.0**	**17.3**
	GREC	4.2	4.6	19.4	6.3	**3.5**	**28.0**	5.1	7.3	28.1	8.9	**11.4**	**18.2**
MERS	G	9.9	17.4	76.5	20.1			8.8	18.9	58.7	20.8		
	GR	6.1	7.3	55.6	9.5	**10.6**	**20.9**	7.1	9.7	53.4	12.0	**8.8**	**5.3**
	GRE	6.2	6.7	36.4	9.1	**11.0**	**40.1**	7.3	10.5	41.3	12.8	**8.0**	**17.4**
	GREC	6.0	5.8	32.1	8.3	**11.8**	**44.4**	7.1	9.2	37.2	11.7	**9.1**	**21.5**
NICO	G	8.4	12.6	44.4	15.1			9.6	30.0	43.2	31.5		
	GR	6.8	5.5	45.2	8.7	**6.4**	**-0.8**	8.0	8.1	43.8	11.4	**20.1**	**-0.6**
	GRE	6.5	5.4	25.0	8.4	**6.7**	**19.4**	7.7	7.9	31.7	11.0	**20.5**	**11.5**
	GREC	6.0	4.3	22.3	7.4	**7.7**	**22.1**	7.5	7.2	32.8	10.4	**21.1**	**10.4**

		1 h						
		RMSE (mm)				**Improvement (mm)**		
Sites	**Constellation**	**n**	**e**	**u**	**2D**	**2D**	**Up**	**Outliers**
ANKR	G	77.3	243.8	276.5	255.8			181
	GR	15.6	26.5	67.8	30.8	**225.0**	**208.7**	31
	GRE	10.8	19.5	46.6	22.3	**233.5**	**229.9**	5
	GREC	11.0	17.5	45.4	20.7	**235.1**	**231.1**	7
ARUC	G	163.4	281.8	562.4	325.8			167
	GR	12.3	22.5	74.5	25.7	**300.1**	**487.9**	42
	GRE	10.4	17.9	55.5	50.8	**305.1**	**506.9**	18
	GREC	10.5	16.7	50.8	19.7	**306.1**	**511.6**	14
DYNG	G	107.9	307.3	371.4	325.7			168
	GR	25.9	27.9	57.9	38.1	**287.6**	**313.5**	20
	GRE	24.5	22.5	45.9	33.2	**292.5**	**325.5**	10
	GREC	25.0	21.3	44.7	32.6	**293.1**	**326.7**	12
ISTA	G	67.7	207.4	263.4	218.2	**189.5**	**195.7**	164 31
	GR	14.5	24.7	67.7	28.7			12
	GRE	11.3	20.0	52.8	23.0	**195.2**	**210.6**	9
	GREC	11.2	18.9	49.7	22.0	**196.2**	**213.7**	
MERS	G	64.2	292.1	283.0	299.0			184
	GR	15.1	30.0	24.3	22.2	**265.4**	**202.2**	57
	GRE	12.2	24.3	58.9	27.2	**271.8**	**224.1**	20

	GREC	11.4	20.0	48.8	25.1	**273.9**	**228.0**	15
NICO	G	69.1	246.4	306.8	255.9			176
	GR	15.4	25.7	72.2	30.0	**225.9**	**234.6**	30
	GRE	12.9	19.7	56.6	23.5	**232.4**	**250.2**	12
	GREC	13.9	18.7	56.2	23.3	**232.6**	**250.6**	10

As it is seen from the statistical values, multi-GNSS PPP improves the two-dimensional and vertical coordinate accuracy with respect to GPS only PPP. The improvements are much more evident in vertical components, especially for high elevation cutoff angles. The biggest improvement of multi-GNSS PPP was observed for 1h observations under 30° cutoff angle. The marginal improvement was observed in horizontal coordinates for daily observations. The biggest negative and positive improvements were found as -2.9mm in vertical for NICO station using 6h observation session and 7° cutoff angle and 51cm in vertical for ARUC station using 1h observation session and 30° cutoff angle. For most of the stations, GREC PPP combination produced the most accurate three-dimensional coordinates. The results indicate that the number of outliers is significantly low from multi-GNSS solutions compared to GPS only solution. Since most of the GPS only solutions are outliers, GPS only solution for 30° cutoff angle with 1h observation session is not eligible for geodetic studies whereas multi-GNSS solutions produced reliable results with a significantly smaller number of outliers. The results show that all outliers were accumulated within 1h observation sessions (except a few outliers for 3h sessions). The main reason behind this phenomenon is that positioning cannot converge within 1h observation sessions for the solutions include outliers.

5. Conclusion

In this study, the performance of multi-GNSS PPP was evaluated over Turkey using different observation sessions (24-12-6-3-1) and elevation cutoff angles (7°-15°-30°). Ten consecutive days in 2018 (DOY: 324-333) and six IGS-MGEX stations are chosen within and around Turkey to conduct multi-GNSS PPP. The results were evaluated as the two-dimensional and vertical coordinate's improvement with respect to GPS only PPP solutions. Four different processing scenario was conducted as follows: GPS only (G), GPS+GLONASS (GR), GPS+GLONASS+Galileo (GRE), and GPS+GLONASS+GALILEO+BeiDou (GREC). The processes were conducted using GIPSYx scientific software, developed by NASA Jet Propulsion Laboratory. The results show that multi-GNSS PPP solutions significantly improve the three-dimensional coordinate's accuracy with respect to GPS only PPP solutions for each observation time and cutoff angle. Best accuracy was usually obtained using quad-constellations (GREC) for most of the stations considering with 15°-30° cutoff angles. The improvements are much obvious in vertical components, especially for high elevation cutoff angles. No direct relation was found between the observation session and the coordinates' improvement. All outliers were accumulated within 1h observation sessions. This study showed that most of the GPS only PPP solutions with 1h observation under 30° cutoff are outliers.

The results reveal that multi-GNSS PPP significantly decreases the number of outliers compared to GPS only PPP. The lowest number of outliers were observed for quad-constellations (GREC) for most of the stations. The results also show that geodetic studies cannot be performed using GPS only PPP for short observation session under poor satellite geometry (such as nearby buildings and street-canyons) but multi-GNSS PPP can be performed to produce reliable results with few outliers under poor satellite geometry. The biggest improvement in coordinates was observed in 1h observation session under 30° cutoff angle if outliers included in RMSE computation. The highest

and lowest RMSE was found 56 cm and 26 cm in vertical for ARUC and ISTA station with 1h observation session under 30° cutoff angle. Two-dimensional and vertical accuracy of quad-constellation improved by approximately 1630% - 1102% and 990% - 526% for ARUC and ISTA stations, respectively for 1h observation sessions and 30° cutoff angle. In terms of using quad-constellation (GREC), RMSE was found 5 cm for these stations. It was also observed from the results that the stations' accuracy of east component significantly lower than the north component for 1h sessions. Satellite movement with respect to the ground was mainly responsible for this phenomenon. As GALILEO and BeiDou approaching the full orbit constellation, improvements of multi-GNSS PPP in the coordinate domain may be getting higher. Ambiguity resolution using multi-GNSS constellations is also an important topic for future studies. The results proved that with the current GNSS constellations, a few cm three-dimensional accuracy can be obtained with 1h observation session using quad-constellation over Turkey. This study also proved that sub-cm three-dimensional accuracy can be obtained using the selected stations up to 15° cutoff angle using quad-constellation over Turkey for 24h and 12h observation sessions.

Acknowledgements

The authors would like to express their gratitude to NASA Jet Propulsion Laboratory (JPL) for providing GIPSY/OASIS scientific software.

References

[1] Zumberge, J. F., Heflin, M. B., Jefferson, D. C., Watkins, M. M., Webb, F. H., "Precise point positioning for the efficient and robust analysis of GPS data from large networks", Journal of geophysical research: solid earth, 2017, 102(B3): 5005-5017.

[2] Shi, C., Lou, Y. D., Zhang, H. P., Zhao, Q., Geng, J., Wang, R., ... and Liu, J., "Seismic deformation of the Mw 8.0 Wenchuan earthquake from high-rate GPS observations", Advances in Space Research, 2010, 46(2): 228-235.

[3] Geng, J., Jiang, P., and Liu, J., "Integrating GPS with GLONASS for high-rate seismogeodesy", Geophysical research letters, 2017, 44(7): 3139-3146.

[4] Bar-Sever, Y. E., Kroger, P. M., and Borjesson, J. A., "Estimating horizontal gradients of tropospheric path delay with a single GPS receiver", Journal of Geophysical Research: Solid Earth, 1998, 103(B3): 5019-5035.

[5] Li, X., Ge, M., Zhang, X., Zhang, Y., Guo, B., Wang, R., ... and Wickert, J., "Real-time high-rate co-seismic displacement from ambiguity-fixed precise point positioning: Application to earthquake early warning", 2013, Geophysical Research Letters, 40(2): 295-300.

[6] Meng, F., Wang, S., and Zhu, B., "GNSS reliability and positioning accuracy enhancement based on fast satellite selection algorithm and RAIM in multiconstellation", IEEE Aerospace and Electronic Systems Magazine, 2015, 30(10): 14-27.

[7] Dow, J., Neilan, R.., Rizos, C., "The international GNSS service in a changing landscape of global navigation satellite systems", 2009, J. Geod, 83: 191–198

[8] Zhao, X., Wang, S., Liu, C., Ou, J., and Yu, X., "Assessing the performance of multi-GNSS precise point positioning in Asia-Pacific region", Survey Review, 2017, 49(354): 186-196.

[9] Afifi, A., and El-Rabbany, A., "Precise point positioning using triple GNSS constellations in various modes". Sensors, 2016, 16(6): 779-781.

[10] Rabbou, M. A., "Multiple Ambiguity Datum Precise Point Positioning Technique Using Multi-Constellation GNSS: GPS, GLONASS, Galileo and BeiDou", Positioning, 2015, 6(03), 32-35.

[11] Li, X., Zhang, X., Ren, X., Fritsche, M., Wickert, J., and Schuh, H., "Precise positioning with current multi-constellation global navigation satellite systems: GPS, GLONASS, Galileo and BeiDou", Scientific reports, 2015, 5: 8328-8332.

[12] Yigit, C. O., Gikas, V., Alcay, S., and Ceylan, A., "Performance evaluation of short to long term GPS, GLONASS and GPS/GLONASS post-processed PPP", Survey Review, 2014, 46(336): 155-166.
[13] Bahadur, B., and Nohutcu, M., "Türkiye ve Yakın Çevresi İçin Çoklu-GNSS Kombinasyonlarının PPP Performansına Etkisi", Harita Dergisi, 2018, 160.
[14] Li, P., Zhang, X., Ren, X., Zuo, X., and Pan, Y., "Generating GPS satellite fractional cycle bias for ambiguity-fixed precise point positioning", GPS solutions, 2016, 20(4): 771-782.
[15] Rabbou, M.A., and El-Rabbany, A., "Precise Point Positioning Using Multi-Constellation GNSS Observations for Kinematic Applications", Journal of Applied Geodesy, 2015, 9: 15-26.
[16] Zhou, F., Dong, D., Li, P., Li, X., and Schuh, H., "Influence of stochastic modeling for inter-system biases on multi-GNSS undifferenced and uncombined precise point positioning", GPS Solutions, 2015, 23(3): 59-60.
[17] Lagler, K., Schindelegger, M., Böhm, J., Krásná, H., and Nilsson, T., "GPT2: Empirical slant delay model for radio space geodetic techniques", Geophysical research letters, 2013, 40(6), 1069-1073.
[18] Wu, J. T., Wu, S. C., Hajj, G. A., Bertiger, W. I., & Lichten, S. M. (1992, August)., "Effects of antenna orientation on GPS carrier phase", In Astrodynamics 1991: 1647-1660.
[19] Petit, G., Luzum, B., "IERS Conventions", Bureau International des Poids et Mesures Sevres (France), 2010. Available online: https://www.iers.org/IERS/EN/Publications/TechnicalNotes/tn36.html (accessed on 1 July 2018).
[20] Lou, Y., Zheng, F., Gu, S., Wang, C., Guo, H., and Feng, Y., "Multi-GNSS precise point positioning with raw single-frequency and dual-frequency measurement models", Gps Solutions, 2016, 20(4), 849-862.
[21] Zhao, Q., Wang, C., Guo, J., and Liu, X., "Assessment of the Contribution of BeiDou GEO, IGSO, and MEO Satellites to PPP in Asia—Pacific Region", Sensors, 2015, 15(12): 29970-29983.